

Reduction on Cogging Torque in Flux-Switching Permanent Magnet Machine by Teeth Notching Schemes

Daohan Wang^{1,2}, Xiuhe Wang², and Sang-Yong Jung¹

¹School of Electronic and Electrical Engineering, Sungkyunkwan University, Suwon 440-746, Korea

²School of Electrical Engineering, Shandong University, Jinan 250061, China

The cogging torque in flux-switching permanent magnet machines (FSPMs) is high due to its unique structure and high air-gap flux density. The cogging torque principle in FSPM is different from that in traditional PM machines, which can not be correctly predicted by analytical consideration. The aim of paper is to present the investigation on cogging torque principle in FSPM by analyzing the flux density distribution and a simple cogging torque reduction technique, i.e., teeth notching. Various kinds of notching schemes and their influence on cogging torque are examined along with instantaneous torque and average output torque at different load conditions. Numerical optimization process combined with finite-element analysis, which gives more preciseness to calculations, is performed to minimize cogging torque. The results show that the cogging torque circle depends on the real flux density distribution in the machine rather than the number of stator/rotor poles and the presented method can greatly reduce the torque ripple at only slight cost of average output torque.

Index Terms—Cogging torque, finite-element analysis (FEA), flux switching permanent magnet machine (FSPM), teeth notching.

I. INTRODUCTION

FLUX switching permanent magnet machine (FSPM) is a new type PM machine emerging in recent years. In FSPM, the high performance PMs are housed circumferentially in armature side, which when combined with the bipolar change of winding flux linkage offer a scope to achieve high flux density and high torque density [1]–[3]. The researches in the literature have revealed that FSPM exhibits significant advantages such as high efficient, high power density, high flux weakening capability, high torque-to-volume ratio, favorable for cooling and high speed operation.

However, the cogging torque in FSPM is relative higher compared to other traditional PM machines due to its unique double salient nature and extremely high flux density caused by the flux focusing effects. Cogging torque does not contribute to electro-magnetic output torque, only results in torque pulsations which represent undesirable vibration and acoustic noise. Relevant investigation has demonstrated that FSPM has critical running torque ripple compared to that in traditional PM machines and the torque ripple is mainly caused by the cogging torque [2], [3], [6], [8]. In this case, cogging torque reduction is the strategic issue to be urgently solved for designing high performance FSPM especially used in accurate position control and servo-driving system.

Concerning the cogging torque reduction, numerous methods have been heavily published in the literature on both radial [8]–[10] and axial type PM machines [11]. However, most of them can not be directly used in FSPM except skewing. In [1], the cogging torque is calculated and measured accounting for the influence of manufacture tolerances cause by mechanically weak module stator structure. Very recently, a rotor axis teeth pairing method is presented in [4] which is suitable for reducing cogging torque with odd number of rotor. This method uses different teeth width of axis stack to offset the cogging torque.

In [7], the harmonic current is injected into the excited winding to compensate the torque ripple from the control viewpoint, which is effective but adds the complex and capacity to the control system and causes additional loss.

In [5] and [6], the teeth notching is mentioned to reduce cogging torque in FSPM by employing two rotor notches, but there are not any studies in the literature which implement different notching schemes which can affect cogging torque, where the designer have an idea to choose the suitable notching scheme. And also, there is no study on the influence of notching schemes on running performance of FSPM, especially on average output torque and transient torque ripple at different load conditions. In addition, the principle of cogging torque occurring in FSPM has not been explained well in the literature. Actually, the principle and characteristics of cogging torque in FSPM is different from that of traditional PM machines due to its unique double salient structure and critical saturation.

In this paper, various kinds of notching schemes both in stator and rotor which can be effective for cogging torque reduction are examined. The parameters of the dummy slots which have influence on cogging torque, including the number of dummy slots both in stator and rotor, dimensions of the dummy slots and notching location are considered as design variables and optimized combined with finite-element analysis (FEA). The cogging torque with different notching schemes are calculated and compared, validating that the presented notching schemes are very flexible and effective to reduce cogging torque in FSPM.

At last, we examined the instantaneous torque ripple and average output torque at different load condition, showing that the method presented in this paper can greatly reduce the torque ripple at rated condition, but only slightly reduce the average output torque.

II. PRINCIPLE ANALYSIS OF COGGING TORQUE IN FSPM

In this paper, the three-phase 12/10 FSPM is used for investigation, which structure is shown in Fig. 1 and detailed design parameters are derived from [3] which are shown in Table I. The initial design FSPM is a practical prototype FSPM which design parameters has been carefully optimized to exhibit high efficiency and torque density [3].

Manuscript received February 29, 2012; revised April 22, 2012; accepted May 08, 2012. Date of current version October 19, 2012. Corresponding author: S.-Y. Jung (e-mail: syjung@ece.skku.ac.kr).

Color versions of one or more of the figures in this paper are available online at <http://ieeexplore.ieee.org>.

Digital Object Identifier 10.1109/TMAG.2012.2200237

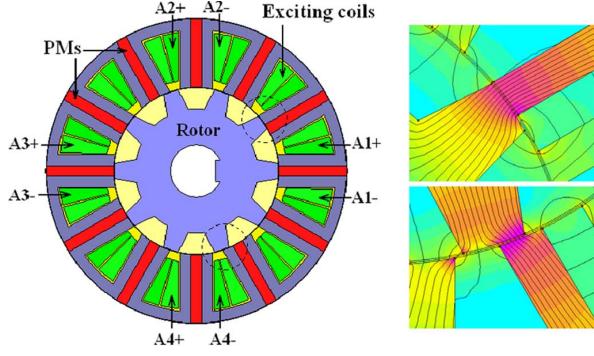


Fig. 1. Schematic of FSPM and flux density.

TABLE I
PARAMETERS OF INITIAL DESIGN FSPM [3]

Parameters	Value	Parameters	Value
Number of stator pole	12	Number of rotor poles	10
Number of phases	3	Rated speed (rpm)	1500
Outer diameter of rotor (mm)	69.8	Inner diameter of rotor (mm)	52
Outer diameter of stator (mm)	128	Coercitive force of PM (kA/m)	950
Length of airgap (mm)	0.35	Material of iron core	DR510
Stack length (mm)	75	Thickness of PM (mm)	4.6
Stator pole arc angle	7.5°	Rotor pole arc angle	10.5°

In an ideal FSPM, the fundamental circle of cogging torque within a rotation period is the least multiple of stator poles and rotor poles, which has been agreed and directly employed in the literatures [1], [5]–[8]. However, this conclusion is obtained from analytical cogging torque analysis used in traditional PM machines. Actually, the analytical method which is able to predict the cogging torque circle in traditional PM machines can not match FSPM with a double salient structure at all.

The cogging torque T_{cog} in FSPM can be expressed as the derivative of the magnetic co-energy W stored in the machine

$$T_{\text{cog}} = -\frac{\partial W}{\partial \alpha} \quad (1)$$

where α is the rotor movement angle. Since the permeability of iron core is much larger than that of the air-gap and PMs, the magnetic co-energy W can be replaced by that stored in the air-gap W_{gap} , ignoring the energy variation in the iron core

$$W \approx W_{\text{gap}} = \frac{1}{2\mu_0} \int_V B^2(\theta) dV = \frac{1}{2\mu_0} \int_V B_r^2(\theta) G^2(\theta, \alpha) dV \quad (2)$$

where θ is the angle along the circumference of air-gap, $B(\theta)$ the flux density distribution in the air-gap along the circumference, $B_r(\theta)$ the flux density distribution generated by PMs in stator, $G(\theta, \alpha)$ the influence of salient rotor on stator flux density. The real situation and analytical prediction for $B_r(\theta)$ and $B_r^2(\theta)$ are shown in Fig. 2. The Fourier expansion of $B_r^2(\theta)$ for the real situation and analytical prediction are shown in (3) and (4), respectively.

$$B_r^2(\theta) = B_{r0} + \sum_{m=1}^{\infty} B_{rm} \cos mP_s\theta \quad (3)$$

$$B_r^2(\theta) = B_{r0} + \sum_{m=1}^{\infty} B_{rm} \cos 2mP_s\theta. \quad (4)$$

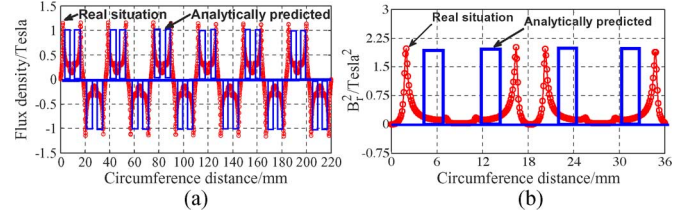
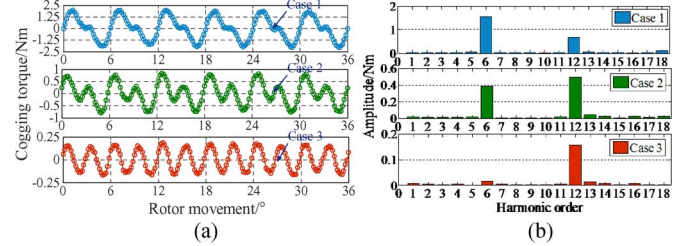
Fig. 2. (a) Distribution of $B_r(\theta)$ and (b) $B_r^2(\theta)$ along the circumference.

Fig. 3. (a) Cogging torque waveforms and (b) harmonic order with three cases.

The Fourier expansion of $G^2(\beta, \alpha)$ is shown as [10]

$$G^2(\theta, \alpha) = G_0 + \sum_{n=1}^{\infty} G_n \cos nP_r(\theta + \alpha) \quad (5)$$

where P_s is the number of stator poles, P_r the number of rotor poles. The cogging torque expression in FSPM can be obtained by substituting (2)–(5) into (1)

$$T_{\text{cog}}(\alpha) = \frac{\pi P_r L_{Fe}}{4\mu_0} (R_2^2 - R_1^2) \sum_{n=1}^{\infty} n G_n B_r \frac{k_{\text{min}}}{P_s} \sin k_{\text{min}} \alpha \quad (6)$$

where L_{Fe} is the axial stack length, R_1 the outer radius of rotor, R_2 the inner radius of stator. According to (6), the cogging torque circle within a rotor rotating period should be the least multiple of P_r and P_s (or $2P_s$), i.e., k_{min}

$$k_{\text{min}} = nP_r = mP_s \text{ or } k_{\text{min}} = nP_r = 2mP_s. \quad (7)$$

According to the real situation of $B_r^2(\theta)$, $k_{\text{min}} = 60$, so the cogging torque circle within a rotor tooth pitch is $k_{\text{min}}/P_r = 6$, whereas, according to the analytical prediction of $B_r^2(\theta)$, $k_{\text{min}} = 120$, so the cogging torque circle is $k_{\text{min}}/P_r = 12$. This is an interesting phenomenon deserving further investigation. Here, we would like to provisionally address that the reason for such a result is mainly due to the extremely high flux density in FSPM, thus analytical method cannot match here. For further study, we established some more FSPM models, which have identical dimensions as the FSPM above but using PMs with shorter length and low energy.

Although having the identical number of stator/rotor poles, the cogging torque circle changes greatly with the three cases as shown in Fig. 3, where Case 1 indicates the initial design and Cases 2 and 3 indicate shorter length and low energy PMs. From Fig. 3, the circle of cogging torque changes from 6 to 12 which agrees well with the analytical prediction above. This is mainly due to the critical saturation and fringing effects in FSPM so that the analytical method can not be used to correctly predict the cogging torque in a normal FSPM which features very high flux density. Hence, the cogging torque circle in FSPM cannot be correctly predicted by just knowing the number of stator/rotor poles, but the real flux density distribution must be needed.

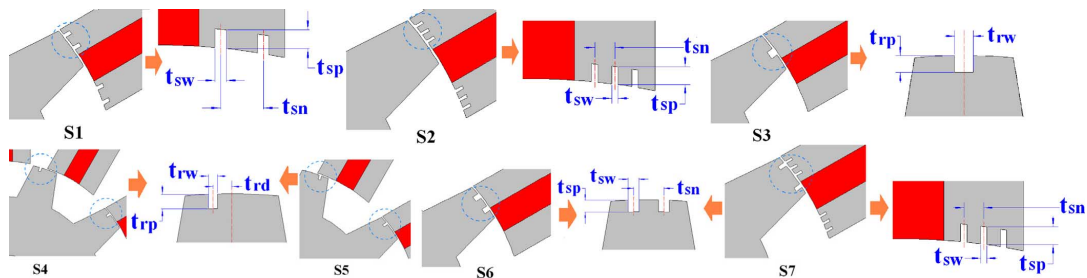


Fig. 4. Notching schemes and design variables (dash zone is the design region).

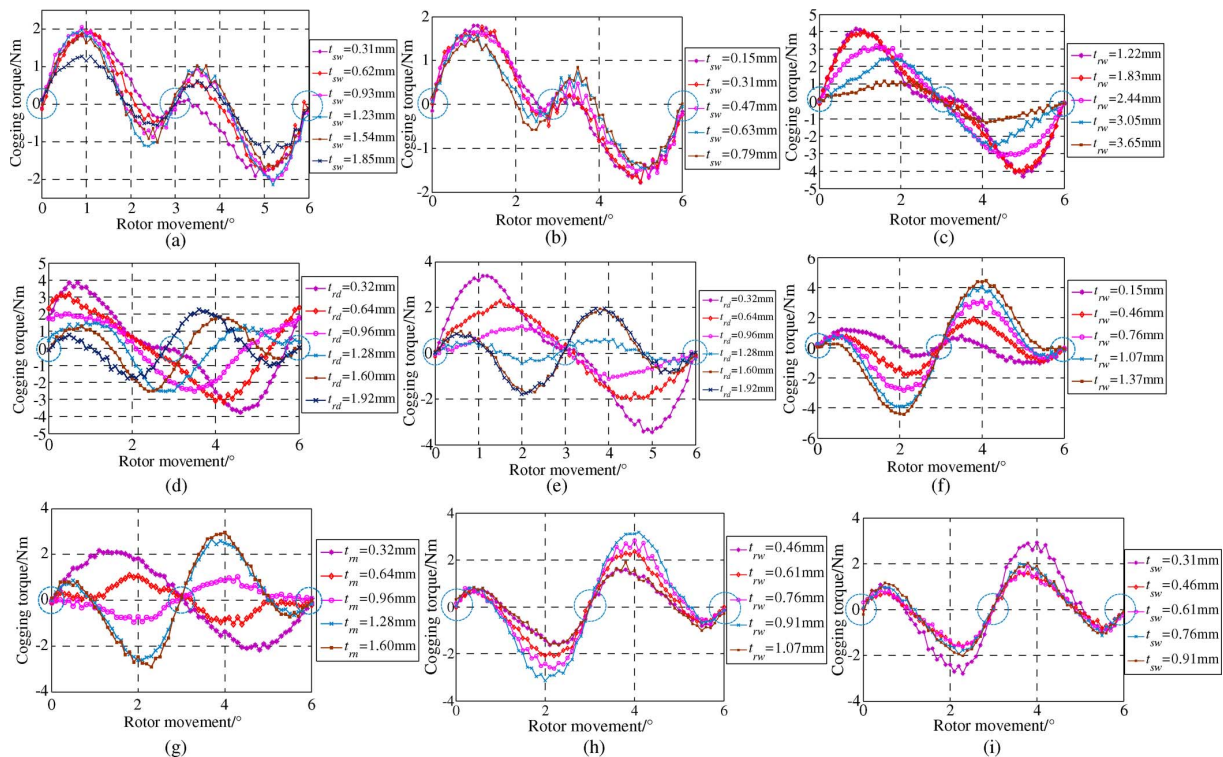


Fig. 5. Cogging torque results obtained by FEA. (a) S1 with t_{sw} variation. (b) S2 with t_{sw} variation. (c) S3 with t_{rw} variation. (d) S4 with t_{rd} variation (t_{rw} is given). (e) S5 with t_{rd} variation (t_{rw} is given). (f) S6 with t_{rw} variation (t_{rn} is given). (g) S6 with t_{rn} variation (t_{rw} is given). (h) S7 with t_{rw} variation (t_{sw} is given). (i) S7 with t_{sw} variation (t_{rw} is given).

Based on the analysis above, we are able to draw a conclusion that if FSPM is manufactured with somewhat tolerances, the cogging torque circle and waveforms will be greatly changed. That is because the cogging torque circle and amplitude is determined by the real flux density distribution in a real machine, which is very sensitive and much more vulnerable to the manufacturing tolerance than that in traditional PM machines due to its “module stator structure.” Also, in practical design, the cogging torque in FSPM should be assessed by FEA or other numerical solutions, which are capable of accounting for the actual dimensions and flux density distribution, rather than using an analytical method.

III. COGGING TORQUE REDUCTION BY TEETH NOTCHING AND NUMERICAL OPTIMIZATION

For reducing cogging torque in FSPM, different notching schemes are examined in this paper, including notching in stator, notching in rotor, both notching in stator and rotor along with different number of notching. Meanwhile, the detailed dimensions and location of the dummy slots which appear to have influence on cogging torque are investigated.

The notching schemes presented in this paper are shown in Fig. 4, which is denoted as S1 to S7, also the design variables of the dummy slots. Note that the influence of dummy slots depth, i.e., t_{rp} and t_{sp} on cogging torque is not crucial, so the value of t_{rp} and t_{sp} are set to be 0.8 mm both considering the mechanical strength and simplifying analysis.

In this paper, the numerical optimization process is combined with FEA to optimize the design parameters for minimizing cogging torque. Fig. 5 shows the cogging torque waveforms with different notching schemes, while the mesh grid, flux density of FSPM and cogging torque results with the optimal design parameters are shown in Fig. 6. It can be seen from Fig. 5(a)–(d) that the peak cogging torque decreases monotonically due to the enlarged air-gap length as the notching widths t_{sw} and t_{rw} increase, which indicates that those schemes S1–S4 have little effect on cogging torque reduction, and the same as scheme S7. The optimal values for different schemes are given in Table II. For most cases, the cogging torque waveforms repeat periodically within 6° despite of a little discrepancy caused by mesh and calculation errors, where the dash zone denote the zero point. However, it does not happen to S4. Hence, the comparison

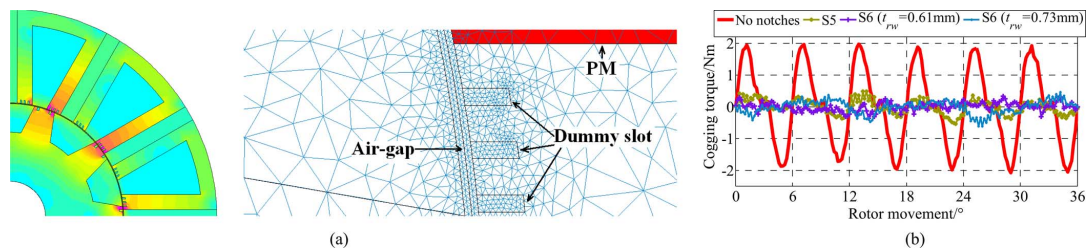


Fig. 6. (a) Mesh grid and flux density calculated by FEA. (b) Calculated results of cogging torque by FEA.

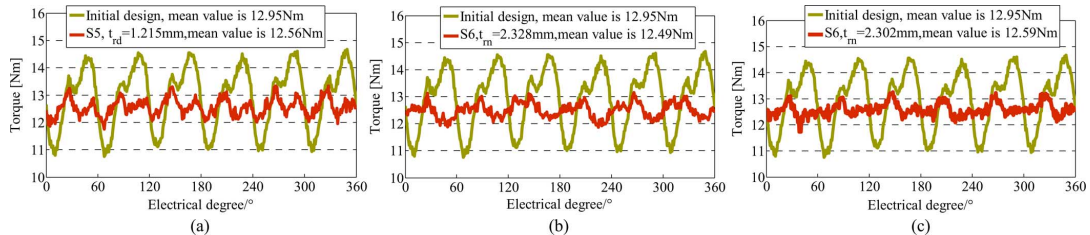


Fig. 7. Instantaneous torque profile with 5A peak current on q -axis. (a) S5, $t_{rd} = 1.215$ mm. (b) S6, $t_{rw} = 0.61$ mm $t_{rm} = 2.328$ mm. (c) S6, $t_{rw} = 0.73$ mm $t_{rm} = 2.302$ mm.

TABLE II
NUMERICAL OPTIMIZATION RESULTS

Notching scheme	S5	S6 ($t_{rw}=0.61$ mm)	S6 ($t_{rw}=0.73$ mm)
Design variables	t_{rd}	t_m	t_m
Optimal values by optimization	1.215 mm	2.328 mm	2.302 mm

of cogging torque should be implemented within a pole pitch of the rotor, i.e., 36° as shown in Fig. 6(b).

IV. INFLUENCE OF THE NOTCHING SCHEMES ON INSTANTANEOUS TORQUE AND TORQUE RIPPLE

For examining the effect of the presented notching schemes on running performance, the instantaneous output torque at rated load conditions are obtained by FEA, which give believable preciseness to calculations. The torque ripple and average output torque are compared to each other with different notching schemes. The results are shown in Fig. 7, validating that the presented method can greatly reduce the torque ripple at only slight cost of average output torque.

V. CONCLUSION

In this paper, the principle of cogging torque in FSPM is investigated. It is found that the cogging torque circle is determined by the real flux density distribution rather than the stator/rotor pole number. Different notching schemes are presented to reduce the cogging torque and optimal dimensions of the dummy slots are determined by numerical optimization. The cogging torque with different notching schemes are compared along with the instantaneous torque profile, average output torque and torque ripple at rated load condition. The results demonstrate that the presented notching schemes can simultaneously reduce the cogging torque and torque ripple at a little cost of average output torque in FSPM.

ACKNOWLEDGMENT

This work was supported by the Basic Science Research Program through the National Research Foundation of Korea

(NRF) funded by the Ministry of Education, Science and Technology (NRF-2012-0003943) and by the Human Resources Development of the Korea Institute of Energy Technology Evaluation and Planning (KETEP) Grant 20114030200030 funded by the Korea government Ministry of Knowledge Economy.

REFERENCES

- [1] Z. Q. Zhu, A. S. Thomas, J. T. Chen, and G. W. Jewell, "Cogging torque in flux-switching permanent magnet machines," *IEEE Trans. Magn.*, vol. 45, no. 10, pp. 4708–4711, Oct. 2009.
- [2] Z. Q. Zhu, J. T. Chen, D. Howe, S. Iwasaki, and R. Deodhar, "Design of multi-tooth flux-switching permanent magnet brushless ac machines for low speed direct drives," *IEEE Trans. Magn.*, vol. 44, no. 11, pp. 4313–4316, Nov. 2008.
- [3] W. Hua, Z. Q. Zhu, M. Cheng, Y. Pang, and D. Howe, "Comparison of flux-switching and doubly-salient permanent magnet brushless machine," in *Proc. 8th Int. Conf. Elect. Mach. Syst. (ICEMS)*, Sep. 2005, vol. 1, pp. 165–170.
- [4] Y. Wang, M. J. Jin, W. Z. Fei, and J. X. Shen, "Cogging torque reduction in permanent magnet flux-switching machines by rotor teeth axial pairing," *Elect. Power Appl. (IET)*, vol. 4, no. 7, pp. 500–506, Jun. 2010.
- [5] W. Hua and M. Cheng, "Cogging torque reduction of flux-switching permanent magnet machines without skewing," in *Proc. 8th Int. Conf. Elect. Mach. Syst. (ICEMS)*, 2008, vol. 1, pp. 3020–3025.
- [6] M. J. Jin, Y. Wang, J. X. Shen, P. C. K. Luk, W. Z. Fei, and C. F. Wang, "Cogging torque suppression in a permanent magnet flux-switching integrated-starter generator," *Elect. Power Appl. (IET)*, vol. 4, no. 8, pp. 647–656, 2010.
- [7] H. Jia, M. Cheng, W. Hua, W. Zhao, and W. Li, "Torque ripple suppression in flux-switching PM motor by harmonic current injection based on voltage space-vector modulation," *IEEE Trans. Magn.*, vol. 46, no. 6, pp. 1527–1530, Jun. 2010.
- [8] N. Bianchi and S. Bolognani, "Design techniques for reducing the cogging torque in surface-mounted PM motors," *IEEE Trans. Magn.*, vol. 38, no. 5, pp. 1259–1265, Sep./Oct. 2002.
- [9] Y.-H. Yeh, M.-F. Hsieh, and D. G. Dorrell, "Different arrangements for dual-rotor dual-output radial-flux motors," *IEEE Trans. Ind. Appl.*, vol. 48, no. 2, pp. 612–622, Mar./Apr. 2012.
- [10] D. Wang, X. Wang, D. Qiao, Y. Pei, and S.-Y. Jung, "Reducing cogging torque in surface-mounted permanent magnet motors by non-uniformly distributed teeth method," *IEEE Trans. Magn.*, vol. 47, no. 9, pp. 2231–2239, Sep. 2011.
- [11] M.-F. Hsieh, D. G. Dorrell, Y.-H. Yeh, and S. Ekram, "Cogging torque reduction in axial flux machines for small wind turbines," in *Proc. 35th IEEE Annu. Conf. Ind. Elect. (IECON)*, 2009, pp. 4435–4439.